Geochemistry Geophysics Geosystems G3
AN ELECTRONIC JOURNAL OF THE EARTH SCIENCES
Published by AGU and the Geochemical Society

Data Brief
Volume 4, Number 7
5 July 2003
1054, doi:10.1029/2002GC000494
ISSN: 1525-2027

Earth's magnetic field in the early 19th century from French sources

Andrew Jackson
Department of Earth Sciences, Leeds University, Leeds LS2 9JT, UK

Also at Department of Earth Sciences, University of Liverpool, Liverpool L69 3GP, UK.

Art R. T. Jonkers
Department of Earth Sciences, Leeds University, Leeds LS2 9JT, UK

Mioara Mandea
Institut de Physique du Globe de Paris, Place Jussieu, Paris, France

Anne Murray
Department of Earth Sciences, Leeds University, Leeds LS2 9JT, UK

[1] We present both a description of a new magnetic data set covering predominantly the 18th and 19th centuries and the results derived from it for the small window 1820–1850, from which the bulk of the data originate. The data set comprises measurements of declination taken overwhelmingly on French naval and hydrographic vessels. A list of the vessels is given for one of the data sets. When augmented by extant inclination measurements, the data are capable of resolving the magnetic field at the core-mantle boundary to a high degree of fidelity and thus are a valuable addition to the data set of historical geomagnetic measurements.

Components: 5641 words, 6 figures, 3 tables.

Keyword: geomagnetism.

Index Terms: 1545 Geomagnetism and Paleomagnetism: Spatial variations (all harmonics and anomalies); 1555 Geomagnetism and Paleomagnetism: Time variations—diurnal to secular.

Received 12 December 2002; **Revised** 24 April 2003; **Accepted** 15 May 2003; **Published** 5 July 2003.

Jackson, A., A. R. T. Jonkers, M. Mandea, and A. Murray, Earth's magnetic field in the early 19th century from French sources, *Geochem. Geophys. Geosyst.*, *4*(7), 1054, doi:10.1029/2002GC000494, 2003.

1. Introduction

[2] In our quest to understand the mechanisms underlying the generation of the Earth's magnetic field, it is desirable to have as long a record as possible of the evolution of the field. On the one hand, palaeomagnetism supplies valuable low-resolution information on the field over timescales of thousands of years to hundreds of millennia, whereas direct measurements of the field can supply much higher spatial resolution, albeit restricted to the last few hundred years. There has recently been much progress in numerical simulation of the geodynamo (for recent reviews, see *Jones* [2000]; *Busse* [2000]; *Zhang and Schubert* [2000]; *Dormy et al.* [2000]; and *Kono and Roberts*

[2002]), and both the observation palaeomagnetic and historical provide important data which can guide the numerical work, at least in a stochastic sense.

[3] We have recently gathered historical data on both global scales [e.g., *Jackson et al.*, 2000; *Jonkers et al.*, 2003] and at single sites [*Alexandrescu et al.*, 1996] in order to improve the fidelity with which we can reconstruct the magnetic field. In the course of these studies we discovered some new sources of magnetic data which we believe are of use to geophysicists, and we describe these data in detail here. These data have previously been used in the work of *Jackson et al.* [2000], although they have not previously been given a full description.

[4] We use the data to reconstruct the magnetic field at the core-mantle interface, a procedure which has previously led to numerous insights. For example, the dynamical effect of the inner core is almost certainly exhibited in the field morphology [*Gubbins and Bloxham*, 1987], and the so-called westward drift has been shown to be a too simplistic view of the secular variation, there being a distinct partitioning between the secular variation of the Pacific and Atlantic hemispheres [*Bloxham and Gubbins*, 1985; *Walker and Backus*, 1996]. The fact that the four large fluxlobes which are quite symmetrically placed about the equator and at high latitudes do not seem to exhibit much displacement over both the historical and palaeomagnetic record has meant that a major question of current interest is whether inhomogeneities in the lower mantle are capable of "locking" the magnetic field, preventing drift which is such a common feature of convection. The period that we analyze here (1820–1850) is too short to yield much new insight into these issues; nevertheless this is part of a much larger data compilation project [see, e.g., *Jackson et al.*, 1997; *Jonkers et al.*, 2003] which will ultimately map the field over the last 500 years with more fidelity than previously.

[5] In section 2 we describe the new data sets and also the assignment of errors which has been performed. Section 3 describes the results of using the data to infer the magnetic field at the core-mantle boundary (CMB).

2. Data

2.1. Scope of the Data

[6] Our primary sources of data are two previously unreferenced manuscripts which reside in the *Archives Nationales* and *Bibliothèque Nationale* in Paris; we refer to these as the AN and BN data sets. Their archival references are respectively ANP MAP 6JJ nos. 80–81, and BNP *Nouvelles Acquisitions Françaises* no. 9,460. The former is believed to have been compiled around 1850, the latter about two decades later. The AN document consists of a set of large sheets of paper, each of which describes a certain latitude/longitude sector of the world, gridded into one-degree squares. Many of the squares carry a magnetic observation, in the form of a date and a declination observation. The source of each datum is unknown, but many of them originate from the French Navy, as attested by the phrase "*Les déclinaisons écrites en l'encre rouge ont été observées abord des batiments chargés de faire de l'hydrographie*," written on two of the sheets. In all, this manuscript contains 9,576 useful measurements; 4,940 data are from the French Hydrographic Service (otherwise known during this period as "Dépot général de la marine") and 4,636 from other French naval sources. Some of the other data (449 points) have been reduced to epoch by the compilers and we do not use them; we believe it is likely that the manuscript was used in the construction of French charts of declination. The charts themselves have not been found. The data from AN are shown in Figure 1. Red dots represent observations made by ships in the *Service Hydrographique*; blue dots represent the other French naval measurements.

[7] The data from the *Bibliothèque Nationale* originated in a book that carries a similar discretization of the world into squares of size 10 minutes. Each datum is a declination observation accompanied by a date. A list of ships, reproduced in Table 1, is provided at the back of the book, and we assume that these are French Naval/Hydrographic Office ships. The names have been reproduced as they

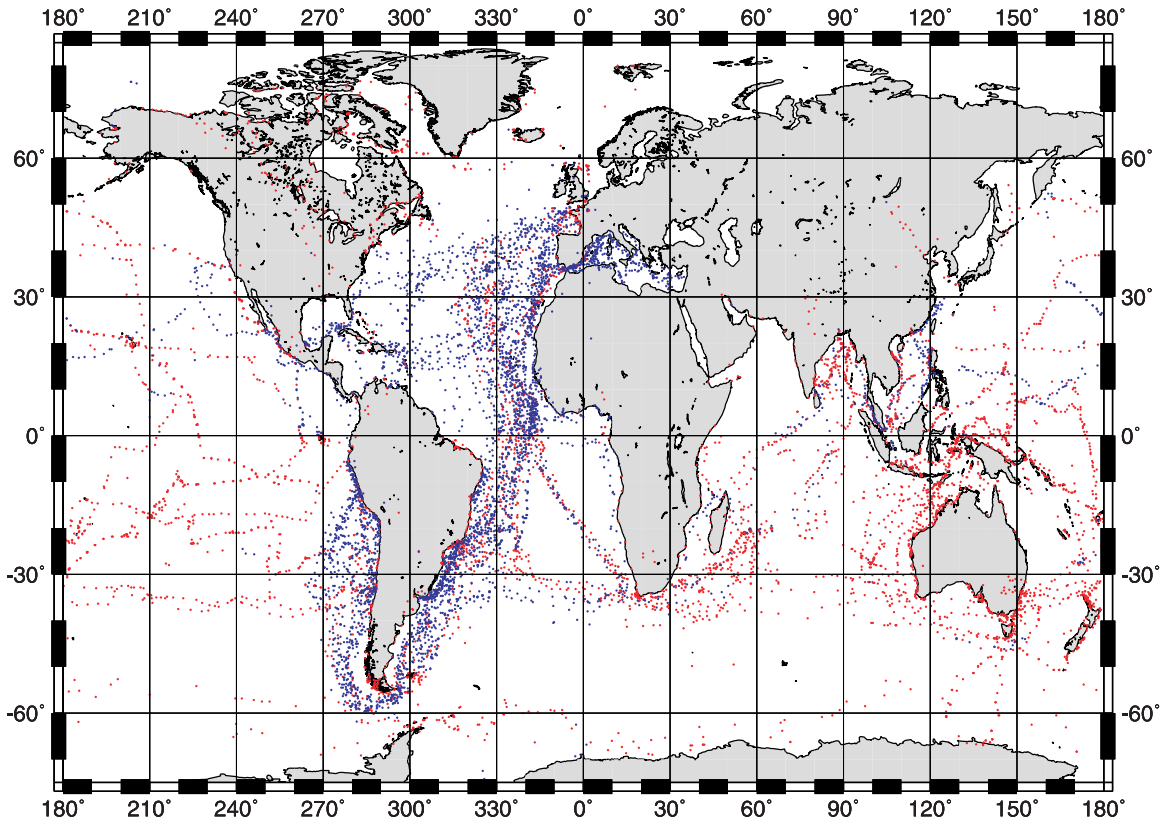

Figure 1. Global distribution of all declination measurements found in the *Archives Nationales* document. Red dots represent observations made by ships in the *Service Hydrographique*; blue dots represent the other French naval measurements. Note in particular the coverage in the Pacific and along South American shores. N = 9,576.

appear in the book, and may be subject to transliteration errors. The data from BN are shown in Figure 2. These clearly show the applied grid.

[8] We have checked each of these data sets, both internally and against one another, to remove duplicate records. In total we found 1,355 identical values, which we removed from the composite AN/BN data set. We have also found that the BN data set contains 354 points from the compilation of *Mountaine and Dodson* [1757] (hereinafter referred to as MD), whose compilation contains 384 data. The effort undertaken by MD was one of the earliest attempts at a global data compilation and provided gridded results at 5 degree intervals over the Atlantic and Indian ocean based on some fifty thousand original measurements from English merchant and naval shipping. Unfortunately, MD published no details of how many data contributed to each value or of how the averaging was performed; their original data compilation has never been found. A greater problem lies in the imperfect navigation of this time period, and we presume that MD were unable to determine navigational imperfections, which could be substantial [see, e.g., *Jackson et al.*, 2000]. These averaged data from MD have been omitted from the data set.

[9] By far the majority of the new data span the period 1820–1850, so this is the period over which we chose to model the magnetic field. Figure 3 shows the temporal distribution of the 1820–50 subset. When combined, the AN and BN data sets supplied a total of 34,958 observations within this time window. But because declination data alone are incapable of determining the magnetic field uniquely, we add to the declination data measurements of inclination from our existing data set [*Bloxham et al.*, 1989]. These comprise 4,667 measurements of inclination, primarily originating in the catalogues of *Sabine* [1872, 1875, 1877] and *Veinberg* [1929]. Table 2 shows the size of each

Table 1. Recorded Ship Names in the BN Data Set

Ship	Period
Abeille	?
Abondance	?
Acheron	1853–55
Adonis	1833, 1837–38, 1840–44
Adour	1828–30, 1838–43
Africaine	1841–44, 1847
Agathe	1836
Aigrette	1829–32
Alcibade	1839
Alcibiade	1826–33
Alcyone	1835–36, 1842
Alerte	1834–35, 1841–42
Algerie	1851–52
Algesina	1829, 1835–36
Algesvias	?
Allier	1832–37, 1841, 1843–44, 1847–48
Alsacienne	1824, 1826, 1828, 1838, 1840
Amaranthe	1819–20
Amazone	1821–23, 1829, 1840
Amphitrite	1824–25
Andromede	1836–37, 1840, 1844–45, 1847
Antigone	1820–22, 1825–28
Archimede	1844–47, 1850, 1852
Arethuse	1825–26, 1828–30, 1841
Argus	1818
Ariane	1834–39, 1844, 1847–48
Armide	1840–42, 1846
Arriege	1825–26
Artemise	1837–40, 1851–54
Artesienne	1825
Arthemise	1852–54
Astree	1822–23, 1826–28, 1834, 1838–39, 1841
Astrolabe	1785–87, 1825–26, 1831, 1835, 1837–40
Atalante	1839, 1841
Atlante	1728, 1730, 1833–34, 1843, 1845
Aube	1836–37, 1840–41, 1843
Aurore	1827–28
Badine	1830, 1832–34, 1836–40
Baucis	1829
Bayadere	1814–15, 1829–30
Bayonnaise	1829, 1833–34, 1847–50
Bearceau	1840, 1842
Bearnaise	1828
Bellonne	1834–35
Berryer(?)	1766–67, 1764–65
Bisson	1835–36, 1838–41
Blonde	1839–40
Bonite	1820–23, 1836–37
Bordelaise	1827–32, 1834, 1837–38
Boudeuse	1768
Bougainville	1835–36
Boussole	1846–48
Brasier	?
Breslaw	1821, 1826
Bressanne	1830
Bressaume	1824–27
Brillante	1839–44
Buciphale	1840–44
Calvados	1859–60

Table 1. (continued)

Ship	Period
Calypso	1831–32, 1841, 1843–44
Camille	1837, 1839–40
Capricieuse	1834–35, 1850–53
Caravane	1834–35, 1838–42, 1844
Caroline	1829–30, 1836
Cassard	1838, 1840, 1845–48
Castor	1847
Cauchoise	1820–22
Cerce	1830–34
Chameau	1825–26
Champenoise	1827–34
Charente	1818–20
Chevrette	1827–29
Chlorinde	1828–29
Cigogue	1827–29
Circe	1823–24, 1833–35, 1838
Colombe	1821–23, 1845
Colosse	1822–23
Comete	1845–46
Constance	1823, 1829–30
Coquette	1843–45
Cormoran	1846
Cornaline	1839–40
Cornilie	1834
Couruline	1841
Cousete	1832
Creole	1832, 1834–36, 1838–41
Cristophe Coloumb	?
Crocodile	1849, 1852
Crocodille	1844–47
Cuirassier	1830–34
Curieux	1821–23
Cygne	1825–28, 1830–33, 1840–41
Danae	1841–43, 1845–47
Daphne	1839–40
Dassa	1839–42
Dauphinoise	1831–32, 1836–38
Desiree	1833
Diane	1824–27, 1829–31
Didon	1837, 1841
Diligente	1824–26, 1830–31
Dolphin	1851–52
Dordogne	1834, 1837
Doris	1842
Dragon	1823–24, 1832, 1844, 1846
Drayer	1859
Dryade	1835–37
Du Petit Thouars	1843–44
Duc De Choisail	1765–66, 1762–64
Duc De Duras	1766–67
Duc De Ventisevre(?)	1764–65
Duchesse De Berry	1819–20
Ducouedie	1830, 1832, 1844, 1846
Duguesne	1828–29
Dunois	1837, 1839–40
Duqueselin	1852
Duquesne	1830
Durance	1822, 1826–32
Eglantine	1841–42, 1845
Egle	1837, 1839
Emulation	1830

Table 1. (continued)

Ship	Period
Endymione	1825–30, 1832
Entrepressam	1849, 1851
Eriton	1846–47
Espadon	1850–52
Esperance	1824–26
Esperence	1821–23
Essafette	1847
Euryale	1822
Eurydice	1823
Expedition	1744
Expedive	1820, 1835–37
Eylan	1824–25
Favorite	1840–44
Fine	1838
Flore	1823–24, 1828, 1835–37
Fortune	1837–44, 1848
Foudroyaur	?
Friedland	1841
Gazelle	1830, 1832, 1837
Genie	1826–28
Girafe	1836–37, 1840, 1847
Gloire	1838, 1840–44
Grenadier	1842–43, 1845–49
Griffon	1837–39, 1844
Guerriere	1822–23
Hebe	1826, 1828–31
Hermione	1832–35, 1838
Hernione	1826–28
Heroine	1830–31, 1844–48
Herome	1836–44
Hussard	1834–37, 1839–42, 1845, 1847
Iena	1839–41
Iguala	1839
Inconstance	1829–31, 1835–36
Inconstant	1838, 1840
Indienne	1843
Iphigenie	1853–55
Isere	1845, 1859–60
Isis	1827–29
Jean-bart	1824–25, 1828–29
Jeanne D'arc	1824, 1830
Jouvencelle	1844, 1846
Jumon	1828
Junon	1830–31
Junon-medee	?
Jupiter	1840–44
Jura	1858, 1860
Kine	?
L'auvergne(?)	1851–55
L'elephant	1764–65, 1817–18
La Beaumoin?	1765–66
La Recherche	1839–40
La Vaiy?	1763–66
La Ville Waul(?)	1765–66
Lana	1847–48
Lancier	1831–32
Laperouse	1841, 1844–47
Laurier	1836–37, 1839–41
Licorne	1840–41
Lilloide	1828–30
Lionne	1837

Table 1. (continued)

Ship	Period
Lizard	1828–34
Loire	1833, 1835–37, 1841, 1844
Lybio	1825–28
Lynx	?
Magicienne	1827–30
Malodine	1839–40
Margueritte	?
Marne	1826, 1829–33
Medee	1830
Meleagre	1853–56
Melecegre?	1848
Melpommene	?
Mercure	1843, 1847
Meteore	1838–40
Meurthe	1843–45, 1847
Minerve	1837–38, 1840
Monstam(?)	1824–25
Moselle	1824, 1826–27, 1830
Naiade	1837–39, 1844–45
Naturaliste	1798, 1803
Neptune	1841–42, 1844
Nereide	1838–39, 1842–44
Neriede	1847
Nievre	1829–36
Ninomernie?	1859–60
Nisus	1829–32, 1840–41, 1843
Nymphe	1824–26
Oise	1834–35
Oreste	1835, 1837–38
Orythie	1830–33
Penelope	1853–55
Prudence	1844–47
Railleuse	1828
Recherche	1835–37, 1844
Resolue	1832
Rhin	1842–46
Ruse	1823–26
Sancier	1823–27
Santi-Petre	1824
Sapho	?
Saphro	1837–38, 1840
Sarcelle	1839–42
Scipion	1840
Seine	1827–28, 1833–34
Shilomele	1832
Sirene	1846
Sirine	1843–45
Sorinde	?
Souffleur	?
Sournee?	1842–46
Spirnie?	1850
St Joseph	1712
Styx	1843–44, 1847
Suffren	1831–32
Surprise	1845–47
Surveillante	1828–30
Sylade	1846
Syrene	1834–37
Syrine	1806
Tactique	1839–40, 1844
Themis	1823–25

Table 1. (continued)

Ship	Period
Therpsichore	1838
Thetis	1822–23, 1828–29, 1839–44, 1847
Thisbe	1832–34, 1838–39
Tigrette	1824–27
Toulormaise	?
Tridente	1823
Triomphante(?)	1839–41
Turquoise	1844
Uranie	1817–20, 1843–44, 1847
Veloce	1838–40
Venthievre?	1766–67
Venus	1824–25, 1828–29, 1841–43
Vestrale	1822–23
Victorieuse	1833–35
Vigie	1841–43
Vigigne	1833–35
Vigogue	?
Vinquem?	1859–60
Virgie	1841–43
Virginie	1844–47
Vottigeur	1838–39
Vottingeur	1841
Zebre	1840–43, 1845

set's contribution for both types of measurement. A full description of these data sets is forthcoming [*Jonkers et al.*, 2003].

2.2. Error Assignment

[10] All the observations in the new data set are of declination. We assign errors to the data from three independent sources: observational (including instrumental) errors, noise due to the crustal field, and errors originating from inaccuracy in position.

[11] For the observational errors, there is considerable evidence as to the accuracy attainable by mariners at sea, at least in the 17th and 18th centuries [*Jonkers*, 2000; *Jackson et al.*, 2000]. During this period, mariners were able to make measurements of declination with a standard deviation of just under half a degree, based on an analysis of repeated measurements on one day. This figure represents the intrinsic accuracy of compasses, coupled with all the other sources affecting the determination such as time-varying

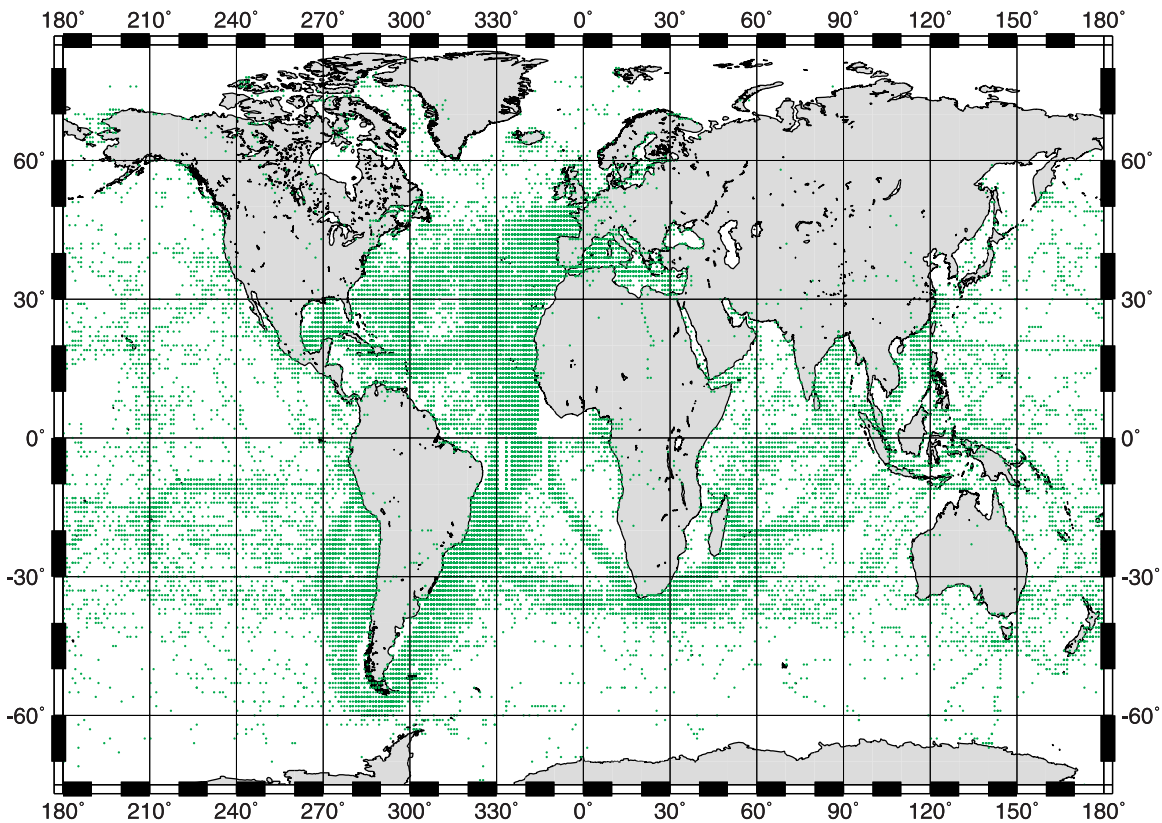

Figure 2. Global distribution of all declination measurements found in the *Bibliothèque Nationale* document, showing the applied grid. N = 35,764.

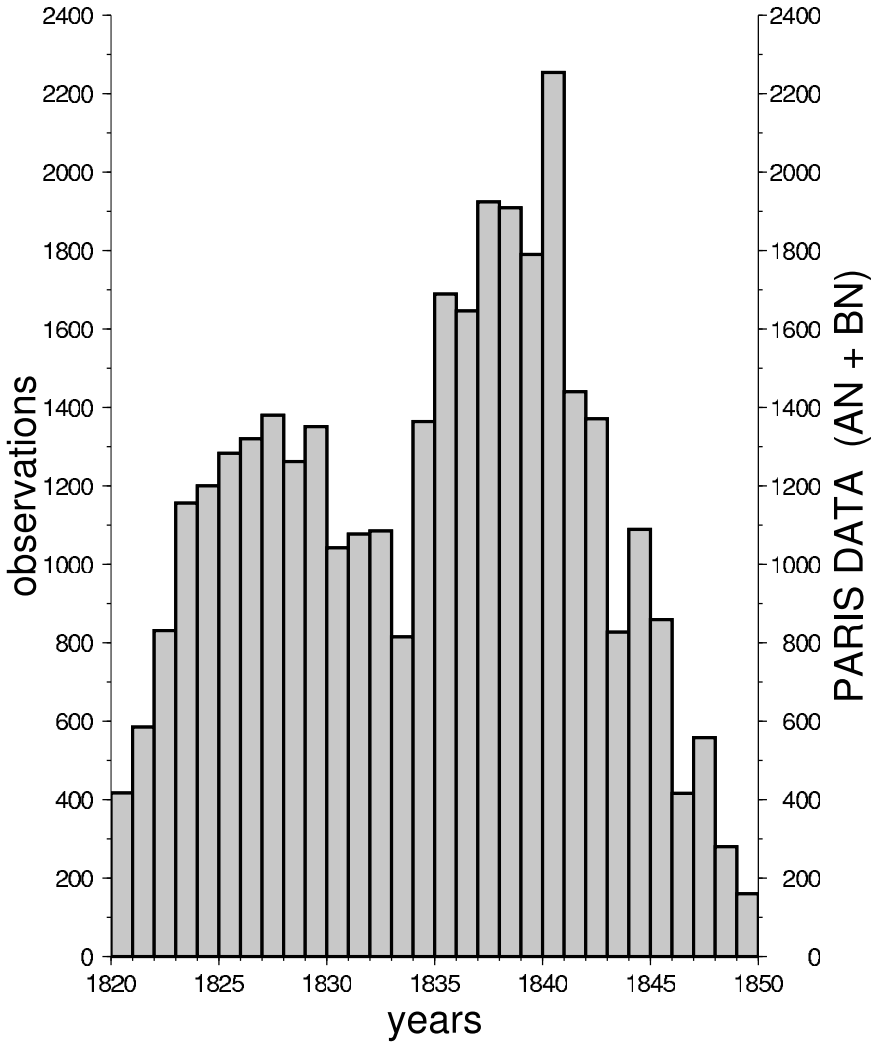

Figure 3. Histogram of the number of declination measurements per year, over the period 1820–1850, as obtained from both Parisian sources. N = 34,958.

external magnetic fields, observational error, and errors in the determination of true north, such as atmospheric refraction (which was well-understood by the 19th century). A potentially more important source of error came into play in the 19th century due to the increased use of iron in ships [*Fanning*, 1986; *Jackson*, 1989]. It was normal practice for the effects of magnetic materials in ships on compass readings to be corrected for as a matter of course, either physically or mathematically through the "swinging" of the ship. We can reasonably assume that this had been carried out on the vessels in the compilation, and that the measurements do not contain systematics due to local magnetic effects.

[12] For the observations of inclination taken at sea there is little objective information available on the reproducibility of such measurements, and we adopt a more pragmatic approach described below.

Table 2. Data Subset Statistics for the Period 1820–1850

Data Set	*D*	*I*	Total
AN	8,422	0	8,422
BN	26,536	0	26,536
Sabine	0	3,961	3,961
Jackson	0	28	28
Veinberg	0	678	678
TOTAL	34,958	4,667	39,625

[13] The errors due to the crust are simply those due to the crustal magnetic field, since this represents a noise source when our target is the core magnetic field. It is unfortunate that the crustal field is not better characterized, however, we adopt the results from stochastic studies of the crustal field which give $\sigma_x = \sigma_y = \sigma \approx \sigma_z/\sqrt{2}$, which seem in accordance with various observations. The values we actually adopt are $\sigma = 200$ nT and $\sigma_z = 300$ nT [e.g., *Bloxham and Jackson*, 1992]; we do not feel that more accurate assignments are warranted. The effect of these fields on measurements of declination and inclination are inversely proportional to the horizontal and total field strengths (H and F respectively, given by model *gufm1* [*Jackson et al.*, 2000]):

$$\sigma_{\text{crust}} = \sigma/H \quad \text{for declination} \tag{1}$$

and

$$\sigma_{\text{crust}} = \sigma_z/F \quad \text{for inclination} \tag{2}$$

This latter error assignment does not account for the slight dependency on inclination as described by *Holme and Jackson* [1997].

[14] During the 19th century, navigation was sufficiently accurate that we will neglect errors due to imprecise location. However, a major contribution to the error budget comes from what might be called digitization or rounding error in the position. The BN data set, as we have already mentioned, is only recorded to an accuracy of one degree in latitude and longitude, and the AN to ten minutes. We were able to check that the procedure for the "binning" is such that the recorded positions represent the center of a box of dimensions $1^\circ \times 1^\circ$ for the AN data set, and therefore the observations had been rounded up or down, as appropriate, rather than merely truncated. The maximum error that this procedure can generate is clearly $\pm 0.5^\circ$, but this will in general be an overestimate of the effect of this procedure on average. Assuming that all positions are equally likely in $[-0.5^\circ, 0.5^\circ]$ about the center of the box, the square root of the expected squared deviation in θ or ϕ is $\sigma_\phi = \sigma_\theta = 1/\left(2\sqrt{3}\right)^\circ$, or approximately 0.29°, only slightly larger than half the maximum error. We use this figure in conjunction with the gradients of the field in the θ and ϕ directions supplied by model *gufm1* [*Jackson et al.*, 2000] to convert the expected positional inaccuracy into an error in the declination, using

$$\sigma_{\text{pos}}^2 = \left(\sigma_\phi \frac{\partial D}{\partial \phi}\right)^2 + \left(\sigma_\theta \frac{\partial D}{\partial \theta}\right)^2 \tag{3}$$

where σ_{pos}^2 signifies the variance of the declination error due to positional inaccuracy. For the BN data set σ_θ and σ_ϕ are reduced by a factor of six because of the reduced box size.

[15] Our final error budget for the declination data is

$$\sigma_{\text{tot}}^2 = \sigma_{\text{pos}}^2 + \sigma_{\text{obs}}^2 + \sigma_{\text{crust}}^2 \tag{4}$$

where σ_{tot} is the total error and $\sigma_{\text{obs}} = 0.5^\circ$. These values are used to fill the appropriate diagonal entries of the error covariance matrix Ce.

[16] Figure 4 shows how the gradients in declination can produce some quite large total error assignments, corresponding to declinations taken around the dip poles, although in general the gradient is somewhat less than a degree of declination per degree of longitude.

[17] For the observations of inclination taken at sea there is little objective information available on the reproducibility of such measurements. The data do not generally suffer from location error as in the case of the AN and BN data sets, and we adopt a pragmatic approach of assigning them errors given by equation (2).

3. Method and Results

[18] For a detailed account of the methods used in generating the geomagnetic field model, see *Jackson et al.* [2000], whose approach we follow closely. Our philosophy for constructing the model of the radial field at the core-mantle boundary is the same as that espoused by *Parker* [1994] in his monograph on inverse theory, namely to determine the simplest model (in terms of roughness, defined below) which is capable of fitting the data to within their error estimates.

[19] The calculations are performed using a spherical harmonic expansion in space and an expansion

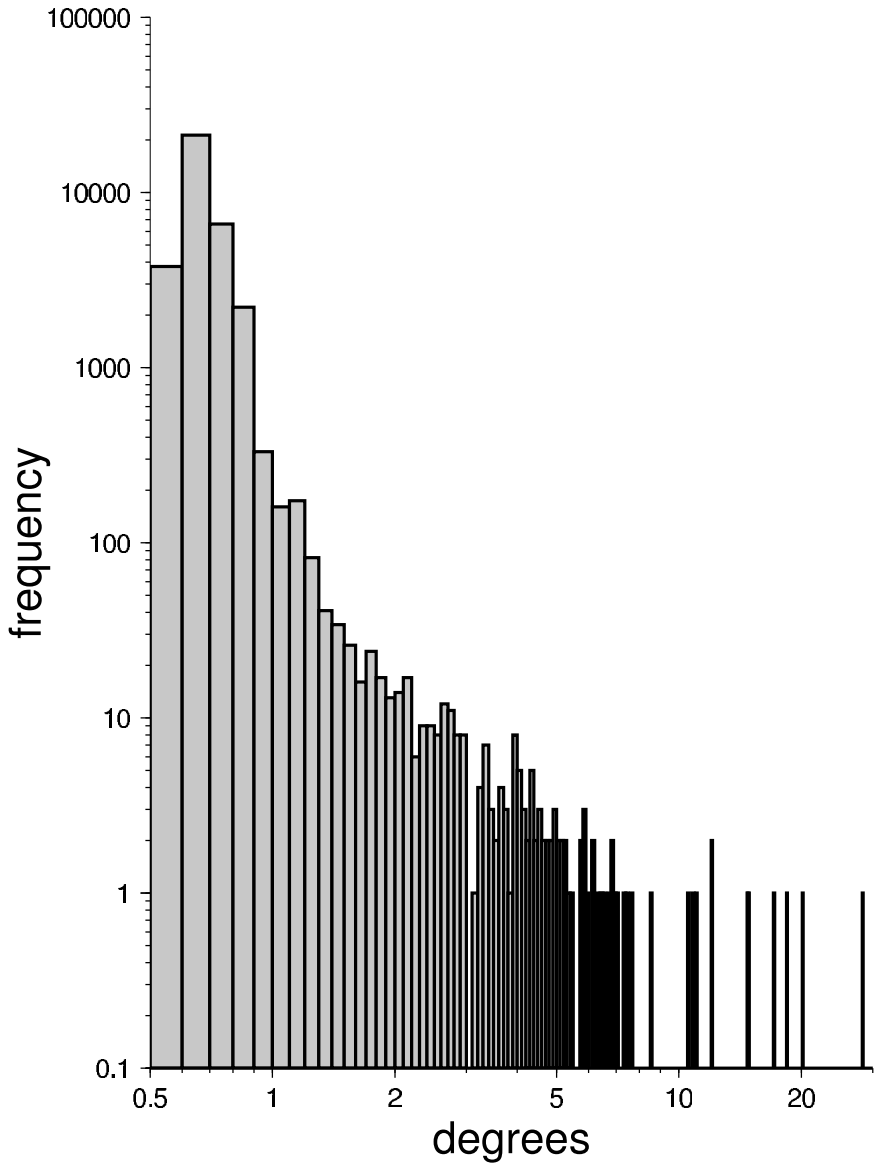

Figure 4. Histogram of error assignments, in degrees, as used in the modeling procedure. Bin width = 0.1 degree; N = 34,958.

of each spherical harmonic coefficient in time in B-splines [*Lancaster and Salkauskas*, 1986], an approach we have found useful previously [*Bloxham and Jackson*, 1992; *Jackson et al.*, 2000]. The spherical harmonic expansion is truncated at degree 14 and the B-splines are erected on knots spaced every 2.5 years, resulting in a set of 3360 coefficients to be solved for. Since no intensities were used in the data set, we fixed the 1840 value at the value of ufm1 [*Bloxham and Jackson*, 1992] at that year (−32265nT) and assigned a dipole decay rate of 15nT/yr.

[20] The data are fit under a quadratic measure of misfit, while minimizing two quadratic norms measuring spatial and temporal complexity; we minimize Θ, where

$$\Theta = [\boldsymbol{\gamma} - \mathbf{f}(\mathbf{m})]^T C_e^{-1} [\boldsymbol{\gamma} - \mathbf{f}(\mathbf{m})] + \lambda_S \mathbf{m}^T \mathsf{S}^{-1} \mathbf{m} + \lambda_T \mathbf{m}^T \mathsf{T}^{-1} \mathbf{m} \quad (5)$$

and where $\boldsymbol{\gamma}$ is the vector of observations, $\mathbf{f}(\mathbf{m})$ is the vector of predictions from the model $\mathbf{m}$, S and T are regularizing matrices described in *Jackson et al.* [2000] and λ_S and λ_T are damping parameters.

Table 3. Statistics of the Model *bnan*

	Value
Number of Data Retained	37654
Number of Data Rejected at 5σ	1970
Misfit	1.97
Damping Parameter λ_S (nT^{-2})	2×10^{-11}
Damping Parameter λ_T (nT^{-2} yr^4)	5×10^{-4}
Spatial Norm Ψ (nT^2)	29×10^{12}
Temporal Norm Φ (nT^2 yr^{-4})	5×10^4
RMS Secular Variation (at CMB) over all years ($nT\ yr^{-1}$)	3300

We use an iterative nonlinear Newton-type algorithm to minimize $\Theta(\mathbf{m})$. We will need to refer to the non-dimensional rms misfit M, defined as

$$M = \sqrt{\frac{1}{N}[\boldsymbol{\gamma} - \mathbf{f}(\mathbf{m})]^T C e^{-1}[\boldsymbol{\gamma} - \mathbf{f}(\mathbf{m})]} \qquad (6)$$

and the spatial and temporal norms Ψ and Φ respectively as

$$\Psi = \mathbf{m}^T S^{-1}\mathbf{m} \quad ; \quad \Phi = \mathbf{m}^T \mathsf{T}^{-1}\mathbf{m}. \qquad (7)$$

In our modeling we found it impossible to fit the data to within one standard deviation on average

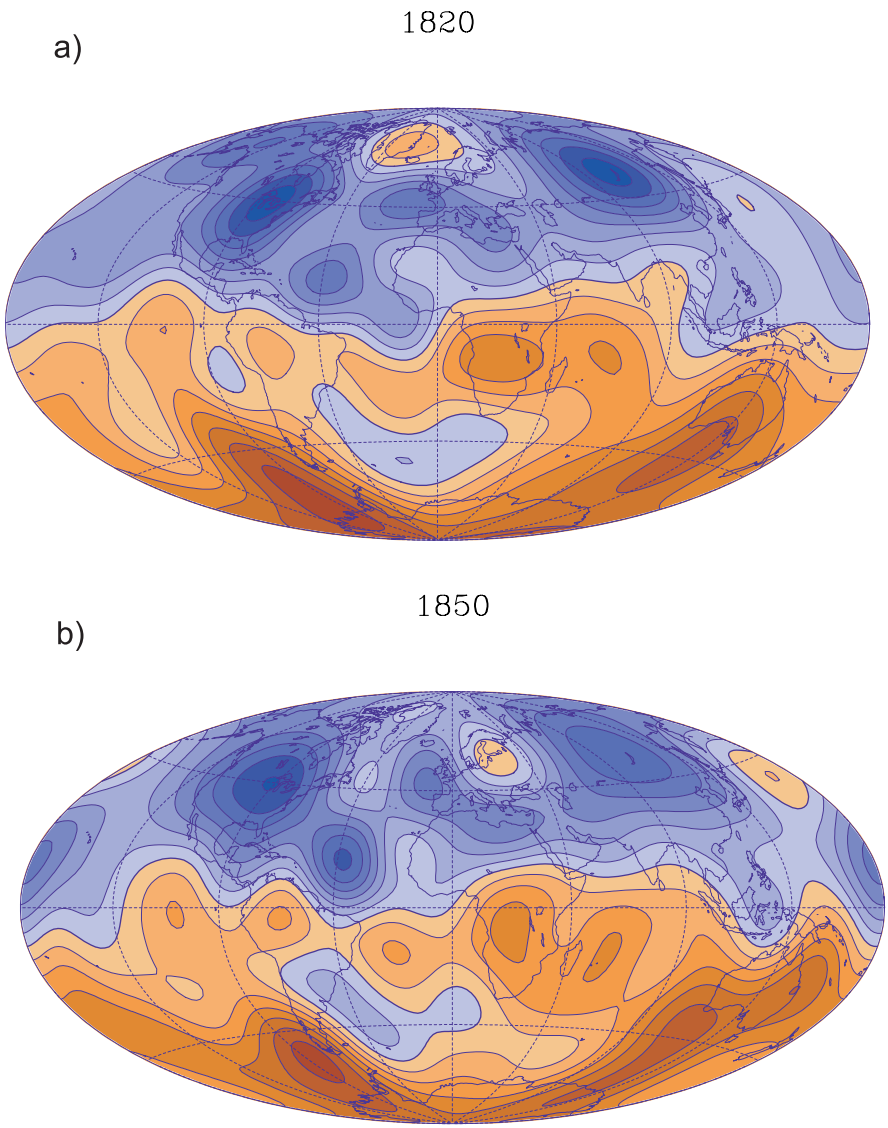

Figure 5. Radial field at the Core-Mantle Boundary for epochs (a) 1820 and (b) 1850. Contour interval is 100 μT, red shades represent radial flux out of the core, blue shades represent flux into the core.

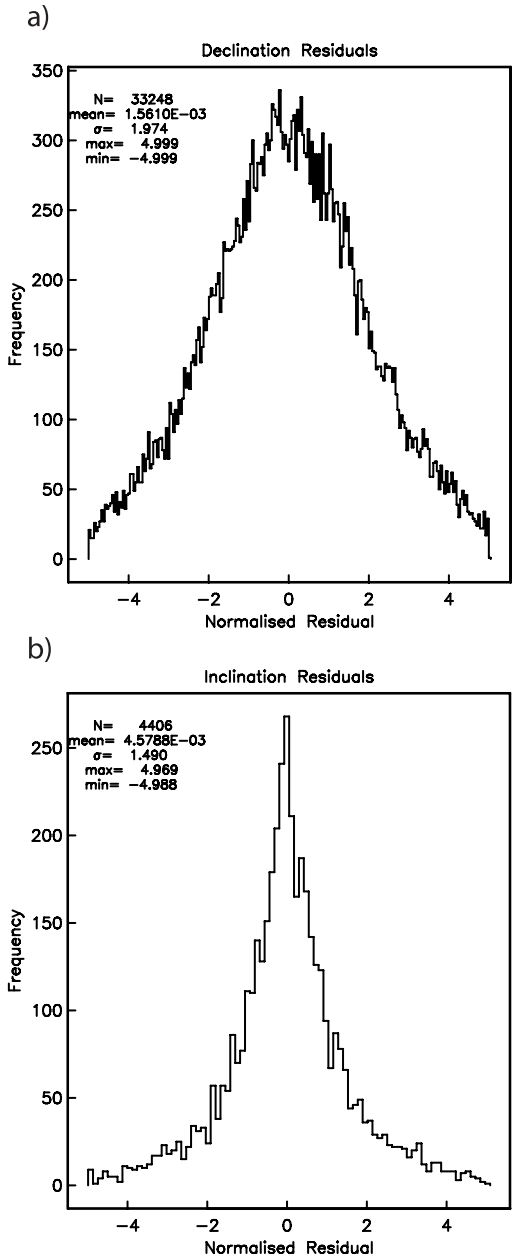

Figure 6. (a) Histogram of weighted residuals from the final model for declination data only. The data have been weighted by their individual error assignments as in Figure 3. (b) Histogram of weighted residuals from the final model for inclination data only. The data have been assigned angular errors of 300nT divided by the local value of the total field intensity at the site.

(a misfit of unity), indicating that our error assignments were too optimistic. We therefore chose λ_S and λ_T so that the two norms Ψ and Φ were approximately 30×10^{12} and 5×10^4 respectively, values consistent with but slightly lower than those attained by *gufm1* [*Jackson et al.*, 2000] over its entire period of validity. Statistics of the final model bnan are given in Table 3.

[21] In Figure 5 we show plots of the magnetic field at the CMB for 1820 and 1850. These show good agreement with previous images [see, e.g., *Jackson et al.*, 2000], albeit at slightly lower resolution. This is to be expected since the amount of data contributing to this model is smaller than that in *gufm1*, and is dominated by declination data, which are known to give suboptimal resolution of some harmonics.

[22] Figure 6 shows histograms of the residuals to the model *bnan*. For the declination data alone we find that the misfit is 1.97; in other words our estimates of the intrinsic errors in the data are roughly a factor of two too optimistic. For the inclination data alone the misfit is 1.49. When we subdivide the 8422 AN data into two sets, one representing the hydrographic part of the data set and one the navy part of the data set (see Figure 1), we find the misfits are 1.86 and 2.09 respectively. This result is in accord with our previous conceptions, namely that the hydrographic service personnel would take more accurate data on average than would the general naval officers.

[23] A more detailed discussion of geomagnetic measurements compiled by European Navies in the 19th century is given by *Jonkers* [2003].

4. Conclusions

[24] We have described a new data set based on archive records held at two of the National Libraries in Paris. These data are of sufficient quality to properly resolve features known to exist in the core magnetic field, and provide a useful addition to the global data set of magnetic measurements. We attempted to objectively assign error estimates to the data, but the data set highlights one of the difficulties of working with historical data, namely that one cannot always know the factors that contribute to the full error budget. Our estimates are a factor of two too small, a large factor compared to our previous success in assigning objective error estimates [*Jackson et al.*, 2000]; it

is possible that the use of iron in the ships of this period, leading to the presence of both induced and remanent magnetization, could contribute to this discrepancy.

[25] Our data are freely available to the scientific community from the World Data Centre for Geomagnetism at the British Geological Survey, Edinburgh, Scotland. It is unfortunate that the bulk of the data are from the period 1820–1850, just outside the time (1850–1860) of a purported magnetic jerk [*Newitt and Dawson*, 1984]. We can only encourage the continued worldwide compilation of historical data, which may ultimately shed light on these types of phenomena prior to the period when a sizable number of observatories began to operate.

Acknowledgments

[26] Some of our figures were prepared using GMT [*Wessel and Smith*, 1991]. AM is grateful to IPG, Paris, for their generous hospitality during the data collection phase.

References

Alexandrescu, M., V. Courtillot, and J.-L. Le Mouël, Geomagnetic field direction in Paris since the mid-sixteenth century, *Phys. Earth Planet. Inter.*, *98*, 321–360, 1996.

Bloxham, J., and D. Gubbins, The secular variation of Earth's magnetic field, *Nature*, *317*, 777–781, 1985.

Bloxham, J., and A. Jackson, Time-dependent mapping of the magnetic field at the core-mantle boundary, *J. Geophys. Res.*, *97*, 19,537–19,563, 1992.

Bloxham, J., D. Gubbins, and A. Jackson, Geomagnetic secular variation, *Philos. Trans. R. Soc. London, Ser. A*, *329*, 415–502, 1989.

Busse, F. H., Homogeneous dynamos in planetary cores and in the laboratory, *Annu. Rev. Fluid Mech.*, *32*, 383–408, 2000.

Dormy, E., J.-P. Valet, and V. Courtillot, Numerical models of the geodynamo and observational constraints, *Geochem. Geophys Geosyst.*, *1*, paper number 2000GC000062, 2000.

Gubbins, D., and J. Bloxham, Morphology of the geomagnetic field and implications for the geodynamo, *Nature*, *325*, 509–511, 1987.

Fanning, A. E., *Steady as She Goes: A History of the Compass Department of the Admiralty*, Her Majesty's Stationery Off., London, 1986.

Holme, R., and A. Jackson, The cause and treatment of anisotropic errors in geomagnetism, *Phys. Earth Planet. Inter.*, *103*, 375–388, 1997.

Jackson, A., The Earth's magnetic field at the core-mantle boundary, Ph.D. thesis, Univ. of Cambridge, Cambridge, England, 1989.

Jackson, A., A. R. T. Jonkers, and A. Murray, Past attractions, *Astron. Geophys.*, *38*, 10–16, 1997.

Jackson, A., A. R. T. Jonkers, and M. Walker, Four centuries of geomagnetic secular variation from historical records, *Philos. Trans. R. Soc. London, Ser. A*, *358*, 957–990, 2000.

Jones, C. A., Convection-driven geodynamo models, *Philos. Trans. R. Soc. London, Ser. A*, *358*, 873–897, 2000.

Jonkers, A. R. T., North by northwest: Seafaring, science, and the Earth's magnetic field (1600–1800), Ph.D. thesis, Free Univ., Amsterdam, 2000.

Jonkers, A. R. T., Geomagnetism, in *Encyclopedia of Maritime History*, edited by J. B. Hattendorf, in press, Oxford Univ. Press, New York, 2003.

Jonkers, A. R. T., A. Jackson, and A. Murray, Four centuries of geomagnetic data from historical records, *Rev. Geophys*, *41*(2), 1006, doi:10.1029/2002RG000115, 2003.

Kono, M., and P. H. Roberts, Recent geodynamo simulations and observations of the geomagnetic field, *Rev. Geophys.*, *40*(4), 1013, doi:10.1029/2000RG000102, 2002.

Lancaster, P., and K. Salkauskas, *Curve and Surface Fitting: An Introduction*, Academic, San Diego, Calif., 1986.

Mountaine, W., and J. Dodson, A letter to the Right Honourable the Earl of Macclesfield, President of the Council and Fellow of the Royal Society, concerning the variation of the magnetic needle; with a set of tables annexed, which exhibit the results of upwards of fifty thousand observations, in six periodic reviews, from the year 1700 to the year 1756, both inclusive; and are adapted to every 5 degrees of latitude and longitude in the more frequented oceans, *Philos. Trans. R. Soc. London*, *50*, 329–350, 1757.

Newitt, L. R., and E. Dawson, Secular variation in North America during historical times, *Geophys. J. R. Astron. Soc.*, *78*, 277–289, 1984.

Parker, R. L., *Geophysical Inverse Theory*, Princeton Univ. Press, Princeton, N. J., 1994.

Sabine, E., Contributions to terrestrial magnetism, no. XIII, *Philos. Trans. R. Soc. London*, *162*, 353–433, 1872.

Sabine, E., Contributions to terrestrial magnetism, no. XIV, *Philos. Trans. R. Soc. London*, *165*, 161–203, 1875.

Sabine, E., Contributions to Terrestrial Magnetism, no. XV, *Philos. Trans. R. Soc. London*, *167*, 461–508, 1877.

Veinberg, B. P., *Catalogue of Magnetic Determinations in USSR and in Adjacent Countries from 1556 to 1926*, Central Geophys. Observ., Leningrad (St. Petersburg), 1929.

Walker, A. D., and G. E. Backus, On the difference between the average values of B_r^2 in the Atlantic and Pacific hemispheres, *Geophys. Res. Lett.*, *23*, 1965–1968, 1996.

Wessel, P., and W. H. F. Smith, Free software helps map and display data, *Eos Trans. AGU*, *72*(41), 445–446, 1991.

Zhang, K., and G. Schubert, Magnetohydrodynamics in rapidly rotating spherical systems*Annu. Rev. Fluid Mech.*, *32*, 409–443, 2000.